Since January 2020 Elsevier has created a COVID-19 resource centre with free information in English and Mandarin on the novel coronavirus COVID-19. The COVID-19 resource centre is hosted on Elsevier Connect, the company's public news and information website.

J Pharmacol Sci **119**, 368 – 380 (2012)

Journal of Pharmacological Sciences

Full Paper

Establishment of Stable Cell Lines With High Expression of Heterodimers of Human 4F2hc and Human Amino Acid Transporter LAT1 or LAT2 and Delineation of Their Differential Interaction With α-Alkyl Moieties

Narakorn Khunweeraphong[1,2,†], Shushi Nagamori[1,†], Pattama Wiriyasermkul[1], Yumiko Nishinaka[1,#], Printip Wongthai[1], Ryuichi Ohgaki[1], Hidekazu Tanaka[1], Hideyuki Tominaga[3], Hiroyuki Sakurai[2], and Yoshikatsu Kanai[1,*]

[1]*Division of Bio-system Pharmacology, Department of Pharmacology, Graduate School of Medicine, Osaka University, 2-2 Yamadaoka, Suita, Osaka 565-0871, Japan*
[2]*Department of Pharmacology and Toxicology, Kyorin University School of Medicine, 6-20-2 Shinkawa, Mitaka, Tokyo 181-8611, Japan*
[3]*Department of Molecular Imaging, Gunma University Graduate School of Medicine, 3-39-22 Showa-machi, Maebashi, Gunma 371-8511, Japan*

Received May 23, 2012; Accepted June 21, 2012

Abstract. System L is a major transport system for cellular uptake of neutral amino acids. Among system L transporters, L-type amino acid transporter 1 (LAT1) is responsible for the nutrient uptake in cancer cells, whereas L-type amino acid transporter 2 (LAT2) is a transporter for non-cancer cells. In this study, we have established HEK293 cell lines stably expressing high levels of human LAT1 and LAT2 forming heterodimers with native human 4F2hc of the cells. We have found that L-[^{14}C]alanine is an appropriate substrate to examine the function of LAT2, whereas L-[^{14}C]leucine is used for LAT1. By using L-[^{14}C]alanine on LAT2, we have for the first time directly evaluated the function of human LAT2 expressed in mammalian cells and obtained its reliable kinetics. Using α-alkyl amino acids including α-methyl-alanine and α-ethyl-L-alanine, we have demonstrated that α-alkyl groups interfere with the interaction with LAT2. These cell lines with higher practical advantages would be useful for screening and analyzing compounds to develop LAT1-specific drugs that can be used for cancer diagnosis and therapeutics. The strategy that we took to establish the cell lines would also be applicable to the other heterodimeric transporters with important therapeutic implications.

Keywords: transporter, amino acid, system L, blood–brain barrier, cancer

Introduction

Amino acid transport across the plasma membrane is mediated via amino acid transporters situated on the plasma membrane. Amino acid transporters were originally described as amino acid transport systems (1). Among them, system L, a Na^+-independent neutral amino acid transport agency, is a major route for living cells to take up neutral amino acids including branched-chain or aromatic amino acids (1). By means of expression cloning, we isolated a cDNA encoding the first isoform of system L transporter named LAT1 (L-type amino acid transporter 1, SLC7A5) (2). Following LAT1, we furthermore identified the second isoform of system L transporter named LAT2 (L-type amino acid transporter 2, SLC7A8) (3). LAT1 or LAT2 forms heterodimers via a disulfide bond with the heavy chain of 4F2 antigen (4F2hc), which is essential for the proper targeting of LAT1 and LAT2 to the plasma membrane (4).

In normal tissues, mRNA of LAT1 has been detected

[†]These authors contributed equally to this work.
[#]Research Fellow of the Japan Society for the Promotion of Science
*Corresponding author. ykanai@pharma1.med.osaka-u.ac.jp
Published online in J-STAGE on July 31, 2012 (in advance)
doi: 10.1254/jphs.12124FP

in brain, ovary, testis, and placenta, whereas its protein has only been reported in the blood–brain barrier and placenta barrier at low levels (2, 4 – 6). LAT1 is now regarded as a cancer cell-type transporter because LAT1 is highly upregulated in malignant tumors and its expression is related to the poor prognosis of patients (7 – 15). LAT1 in cancer cells is, thus, supposed to provide cancer cells with neutral amino acids including several essential amino acids for nutrition (14, 16, 17). The LAT1-specific high-affinity inhibitor has been developed and its antitumor effect has in fact been demonstrated in experimental animals (18). LAT1 can also be involved in the tissue- and cellular delivery of amino acid-related drugs. Anti-Parkinson drug L-DOPA, anticonvulsant gabapentin, and antitumor phenylalanine mustard melphalan are the substrates of LAT1 (15, 19, 20). L-DOPA and gabapentin are supposed to be delivered to the brain by LAT1 at the blood–brain barrier, whereas LAT1 contributes to transport of melphalan to cancer cells (15, 19 – 21). Recently it has been proposed that L-[3-^{18}F]fluoro-α-methyltyrosine, a radiotracer of positron emission tomography (PET) for cancer diagnosis, and borono-phenylalanine for boron neutron capture therapy are accumulated in cancer cells by LAT1 expressed in cancer cells (22 – 24), indicating further applications of LAT1 to cancer diagnosis and therapeutics. In contrast, LAT2 is a normal cell-type transporter widely expressed in an animal body including the small intestine, kidney, brain, placenta, ovary, testis, skeletal muscle, and pancreas (3, 4, 15, 25). In the epithelia of small intestine and renal proximal tubules, LAT2 is localized at the basolateral membrane and responsible for the transepithelial absorption of amino acids from the luminal fluid to blood (25, 26). LAT2 as well as LAT1 participates in the permeation of amino acids and amino acid–related drugs such as L-DOPA through the blood–brain barrier and placenta barrier (27 – 30). One of the notable differences in the substrate selectivity of LAT1 and LAT2 lies in the acceptance of α-methyl moieties. LAT1 accepts α-methyl-L-tyrosine, α-methyl-L-phenylalanine, and α-methyl-L-DOPA as substrates, whereas LAT2 shows less interaction with these aromatic α-methyl amino acids (21, 30, 31).

The chemical compounds targeting LAT1 and avoiding the interaction with LAT2 are, thus, proposed to be drug candidates for cancer diagnosis and therapeutics. Recently, it has been shown that LAT2 is upregulated in some non-cancer lesions (32). Thus, LAT2-specific inhibitors might also be considered therapeutically. To develop such drugs and screen chemical compounds, it is essential to establish in vitro simple assay systems to analyze the interaction with LAT1 and LAT2 separately. However, establishing cell lines stably expressing heterodimeric transporters such as LAT1 and LAT2 suffers from some difficulties. Firstly, most of the host cell lines originally express endogenous LAT1-4F2hc heterodimeric complex, so that the overexpressed exogenous LAT1 or LAT2 has to expel endogenous LAT1 to form heterodimers with 4F2hc to appear on the cell surface. Because the amount of endogenous 4F2hc limits the level of cell surface expression of exogenous LAT1 or LAT2, it would be difficult to obtain high level of functional activity even on overexpression of LAT1 or LAT2. Secondly, because host cells or mock cells exhibit high level of system L activity due to the endogenous LAT1-4F2hc heterodimer, it is difficult to distinguish exogenously introduced LAT1 or LAT2 from endogenous LAT1 activity.

We previously generated mouse S2 cell lines stably expressing human LAT1 (S2-hLAT1 cell) and human LAT2 (S2-hLAT2 cell) (30). The S2 cell was chosen because it was an easy host cell to establish stably transfected cell lines (33). To evaluate the expressed functions, we used L-[^{14}C]leucine as a substrate for both LAT1 and LAT2 because L-leucine is a common substrate for LAT1 and LAT2. L-[^{14}C]leucine uptakes in the S2-hLAT1 and S2-hLAT2 cells measured in Na^+-free medium were supposed to be mediated by exogenously expressed human LAT1 and human LAT2, respectively (30). Although the contribution of LAT1 to L-[^{14}C]leucine uptake of S2-hLAT1 cells has been confirmed by LAT1-specific inhibitor KYT0353 (18), that of LAT2 to L-[^{14}C]leucine uptake of S2-hLAT2 cells has not been proved directly because LAT2-specific inhibitors are not available for the moment. Additionally, S2 cell requires various growth factors and less common culture medium for maintaining (30), so that it is not desirable for large-scale screening of chemical compounds. Further concern on the S2-hLAT1 and S2-hLAT2 cells is that the exogenously introduced human LAT1 or human LAT2 forms heterodimers with endogenous mouse 4F2hc. In this study, to overcome such disadvantages of S2-hLAT1 cells and S2-hLAT2 cells, we have used conventional HEK293 (Human Embryonic Kidney 293) (34) as a host cell to establish new cell lines stably expressing high levels of human LAT1 and human LAT2 and searched for more appropriate substrates to evaluate LAT2 function compared with L-[^{14}C]leucine. Additionally, using newly established and validated cell lines and assays, we have examined the differential interaction of LAT1 and LAT2 with α-alkyl moieties by introducing wider spectrum of compounds.

Materials and Methods

Chemicals

All chemicals used in this study were of analytical

grade. General chemicals were purchased from Wako (Osaka). Amino acids and their related compounds were purchased from Sigma-Aldrich (St. Louis, MO, USA). L-[^{14}C]Leucine and L-[^{14}C]alanine were obtained from Moravek Biochemicals (Brea, CA, USA). The chemical structures of amino acid derivatives used in this study are shown in Fig. 1.

Establishment of stably transfected cell lines

HEK293 cells were obtained from HSRRB (Osaka) and maintained in Minimum Essential Medium (MEM, Wako) containing 10% (v/v) heat-inactivated fetal bovine serum (Invitrogen, San Diego, CA, USA) supplemented with Non-Essential Amino Acid (Wako) under humidity with 5% CO_2 at 37°C. The full-length cDNAs for human LAT1 (GenBank/EMBL/DDBJ accession no. AB018009) and human LAT2 (GenBank/EMBL/DDBJ accession no. AB037669) were subcloned into pcDNA3.1(+), a mammalian expression vector (Invitrogen), to obtain pcDNA3.1(+)-hLAT1 and pcDNA3.1(+)-hLAT2, respectively. HEK293 cells were seeded onto a 60-mm dish at a density of 2×10^5 cells/dish and cultured for 36 h. At 60% – 70% confluence, cells were transfected with 3 μg of pcDNA3.1(+) vector, pcDNA3.1(+)-hLAT1, or pcDNA3.1(+)-hLAT2 by using Lipofectamine™ 2000 (Invitrogen) according to the manufacturer's instructions. At 48 h after transfection, cells were subcultured into a 10-cm plate containing the culture medium supplemented with G418 (0.9 g/l). Cells were seeded at range between $0.5 – 100 \times 10^4$ cells per plate to obtain individual colonies. The culture medium was changed every 2 days for 2 – 3 weeks until the single colony was visualized. Once the colony was formed, a single colony was isolated by using a cloning cylinder. Cells in the isolated clone were trypsinized for 3 – 5 min. Then, the cells were transferred into a 24-well plate containing 500 μl of the culture medium supplemented with G418. The cells were subcultured into a 6-well plate and subsequently 10-cm plates and maintained in the presence of G418.

L-[^{14}C]Leucine uptake was measured for 30 clones of HEK293-hLAT1 cells stably expressing human LAT1 and 20 clones of HEK293-hLAT2 cells stably expressing human LAT2. Among the clones tested, a few clones that showed higher L-[^{14}C]leucine uptake compared with HEK293-mock cells stably transfected with vector plasmid were selected. The final selection relied on the stability of the uptake activities after 10 passages. HeLa S3 cells and S2 cells were cultured as described elsewhere (24, 30, 35)

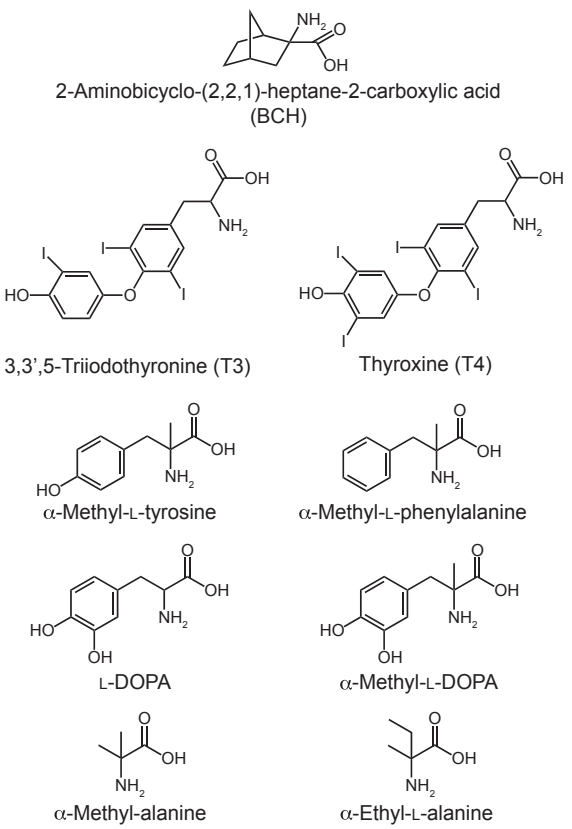

Fig. 1. Chemical structures of amino acid derivatives used in this study.

Reverse transcription polymerase chain reaction (RT-PCR)

To isolate total RNA, cells were cultured as a monolayer in a 10-cm dish to confluence. Cells were washed with PBS and lysed in 1 ml of ISOGEN (NIPPON GENE, Tokyo). RNA isolation was performed following the manufacturer's instructions. The first-strand cDNA from the stable cell lines were generated by utilizing SuperScript™ III Reverse Transcriptase (Invitrogen). The specific primers designed to correspond to the sequences of LAT1, LAT2, LAT3 (GenBank/EMBL/DDBJ accession no. NM_003627.4), LAT4 (GenBank/EMBL/DDBJ accession no. NM_152346), 4F2hc (GenBank/EMBL/DDBJ accession no. AB018010), and GAPDH (glyceraldehyde-3-phosphate dehydrogenase) (GenBank/EMBL/DDBJ accession no. NM_002046) are as follows: LAT1 Fw, 5′- CGG TTC CCC GCA ACC CAC -3′; LAT1 Rv, 5′- AGG AGT CCA TCG GGG CCT C -3′; LAT2 Fw, 5′- TCC CCA TCA TAC CTG CAC CCA -3′; LAT2 Rv, 5′- TGC CCC AAG ACA GCA TGA CAC -3′; LAT3 Fw, 5′- GAA GCC TTT CCT GCC CCT GAG -3′; LAT3 Rv, 5′- CTA TGC GGT CAC CTC AGA GCC -3′; LAT4 Fw, 5′- GAG GAC ATG GAC TAC TCG GTG -3′; LAT4 Rv, 5′- CTA CAC GAA GGC CTC CTG GT -3′ ; 4F2hc Fw, 5′- ATG AGC CAG GAC ACC GAG GT -3′; 4F2hc Rv, 5′- GCG CAA GCT TTC AGG CCG CGT AGG GGA AG -3′, GAPDH Fw, 5′- TGG AAA

TCC CAT CAC CAT CT -3′; GAPDH Rv, 5′- GTC TTC TGG GTG GCA GTG AT -3′. The PCR reactions were conducted by using KOD FX (Toyobo, Osaka) with the cDNA template according to the following protocol: 98°C (10 s), 60°C (30 s), 68°C (60 s); 15 cycles. The PCR products were analyzed on agarose gel electrophoresis.

Membrane preparation and western blot analysis

For crude membrane preparation, cells cultured on 10-cm plates to confluence were collected and suspended in 500 μl buffer containing 50 mM Tris-HCl (pH 7.4), 150 mM NaCl, 5 mM EDTA, 1 mM phenylmethylsulfonyl fluoride, 1 mM Na_3VO_4, and 1 mM NaF. Cells were then disrupted by ultra-sonication in ice-cold water. Cell debris was separated by centrifugation at 1,000 × *g* for 5 min at 4°C. The supernatants were ultracentrifuged at 45,000 × *g* for 30 min at 4°C. After the centrifugation, the crude membrane pellet was lysed with 50 mM Tris-HCl (pH 7.4), 150 mM NaCl, 1 mM EDTA, 1 mM phenylmethylsulfonyl fluoride, and 1% NP-40. The protein concentrations were measured by BCA protein assay (Thermo Fisher Scientific, Waltham, MA, USA). The lysates were mixed with the Laemmli sample buffer with (reducing condition) or without (non-reducing condition) 100 mM dithiothreitol (DTT) and then subjected to SDS-PAGE.

Plasma membrane fractions were prepared as described previously (36) with minor modification. The cell pellet was suspended in homogenization buffer containing 10 mM Tris-HCl (pH 7.5), 250 mM sucrose, 100 mM NaCl, 1 mM EDTA, and Protease inhibitor cocktail (Roche Applied Science, Indianapolis, IN, USA). The cells were homogenized and centrifuged at 1,000 × *g* for 5 min at 4°C. The supernatants were centrifuged at 430,000 × *g* in a Hitachi S100AT4 rotor (Hitachi Koki, Tokyo) for 15 min and the membrane pellet was resuspended in 0.75 ml of 30% iodixanol solution [20 mM Tris-HCl (pH 7.5), 1 mM EDTA, 30% (w/v) iodixanol (Axis-Shield PoC AS, Oslo, Norway), 125 mM sucrose]. The membrane suspension was overlayed by 3 ml each of 25%, 17.5%, 10%, and 2.5% iodixanol solutions sequentially and centrifuged at 100,000 × *g* in a Beckman SW41 Ti rotor (Beckman Coulter, Brea, CA, USA) for 16 h. One milliliter of each fraction was collected from the top. All fractions were analyzed by SDS-PAGE and western blotting. After confirmation by western blotting with plasma membrane markers or organelle markers, fractions from the 2.5% – 10% iodixanol interface were pooled as the plasma membrane fraction. The protein concentrations were measured by BCA protein assay. The membrane fractions were dissolved in 1% Fos-Choline-12 (Affymetrix, Santa Clara, CA, USA), mixed with the Laemmli sample buffer, and subjected to SDS-PAGE.

After SDS-PAGE, the separated proteins were transferred electrophoretically to a Hybond-P PVDF transfer membrane (GE Healthcare Life Sciences, Pittsburgh, PA, USA). The membrane was pre-blocked in blocking solution [5% (w/v) skim milk] at room temperature for 1 – 2 h. The membrane was then incubated with the blocking solution containing 1:10,000 dilution of antibody, either affinity-purified rabbit anti-LAT1 *C*-terminus polyclonal antibody (19), rabbit anti-LAT2 antiserum against amino acid residues from 505 to 516 (30), or anti-CD98 (H300) antibody against 4F2hc (Santa Cruz Biotechnology, Santa Cruz, CA, USA). The membrane was treated with horseradish-peroxidase-conjugated anti-rabbit IgG (Jackson ImmunoResearch Laboratories, West Grove, PA, USA) as the secondary antibody. The signal was developed by using Immobilon Western Chemiluminescent HRP Substrate (Millipore, Billerica, MA, USA) and visualized under the LAS-4000 mini Luminescent image analyzer (Fujifilm, Tokyo).

Co-immunoprecipitation

The cells were harvested from a 10-cm dish and lysed in the lysis buffer [50 mM Tris-HCl pH 7.4, 150 mM NaCl, 1 mM EDTA, 1% Triton X-100, and Protease Inhibitor Cocktail (Roche Applied Science)]. The cell lysates were incubated overnight at 4°C with either control mouse IgG (Santa Cruz) or anti-4F2hc monoclonal antibody HBJ127 (37) provided by Dr. Yasuhiko Ito, Chubu University. The lysates were mixed with Dynabeads protein G (Invitrogen) and incubated for 1.5 h with rotation at 4°C. The beads were washed with the lysis buffer and resuspended in the Laemmli sample buffer. The samples were heated at 65°C for 10 min and then subjected to SDS-PAGE. The separated proteins were detected by western blotting as described above.

Uptake experiments

The functional clones of stable cell lines were analyzed in the uptake experiments as described previously (30, 38). Briefly, HEK293-mock, HEK293-hLAT1, and HEK293-hLAT2 cells were seeded at the density of 1×10^5 cells/well onto collagen-coated 24-well plates. The cells were used for the uptake experiments two days after seeding when the cells reached to approximately 90% – 100% confluence. After removal of the culture medium, the cells were carefully washed with pre-warmed Na^+-free HBSS (Hank's balance salt solution) containing 125 mM chlorine chloride, 4.8 mM KCl, 1.2 mM $MgSO_4$, 1.2 mM KH_2PO_4, 1.3 mM $CaCl_2$, 5.6 mM glucose, and 25 mM HEPES (pH 7.4) and then pre-incubated in 500 μl of pre-warmed Na^+-free HBSS at 37°C for 10 min before adding substrates for the uptake experi-

ment. The cells were then incubated at 37°C for 1 min in 250 μl of uptake medium: Na^+-free HBSS containing L-[^{14}C]leucine (5.0 MBq/mmol) or L-[^{14}C]alanine (5.0 MBq/mmol). Subsequently, the cells were washed three times with ice-cold Na^+-free HBSS. The cells were then lysed with 500 μl of 0.1 N NaOH and the lysate was mixed with 3.5 ml of Emulsifier safe cocktail (PerkinElmer, Waltham, MA, USA). The radioactivity was measured by a β-scintillation counter (LSC-3100; Aloka, Tokyo). For the inhibition experiments, the uptake of 1 μM L-[^{14}C]leucine or L-[^{14}C]alanine was examined in the presence or absence of 1 mM non-radiolabeled test compounds. For T3 and T4, 10 μM of the compounds with 0.1% DMSO were used to examine their inhibitory effect on the uptake of L-[^{14}C]leucine and L-[^{14}C]alanine (1 μM) due to the low solubility of the compounds. The uptake was measured for 1 min because it was within the linear rage of the time dependent uptake of L-[^{14}C]leucine and L-[^{14}C]alanine. To obtain K_m and V_{max} values of the transport, the uptake of substrate was measured at 1, 10, 100, 300, 500, 1,000, 1,500, and 2,000 μM. Kinetic parameters, K_m, V_{max}, and K_i, were determined by a non-linear regression program in SigmaPlot 11 (Systat Software, Chicago, IL, USA).

All experiments were performed with 3 – 5 replications. The data are expressed as means ± S.E.M. Statistical differences were determined using the unpaired Student's *t*-test. Differences were considered significant at $P < 0.05$.

Results

Expression of LAT1 and LAT2 in cell lines

The human cell lines established in this study, HEK293-hLAT1 and HEK293-hLAT2, stably expressing human LAT1 and human LAT2, respectively, were cloned under the selections for higher uptake of L-[^{14}C]leucine compared with the HEK293-mock cells and also for the stability of L-[^{14}C]leucine uptake after 10 passages. Expression of system L transporters, LAT1, LAT2, LAT3, and LAT4, in HEK293-mock, HEK293-hLAT1, and HEK293-LAT2 cells was examined by RT-PCR (Fig. 2A). mRNA for endogenous LAT1 was slightly detected in the mock cells (lane 1) and HEK293-LAT2 cells (lane 13), whereas LAT1 expression in HEK293-hLAT1 cells was significant (lane 7). LAT2 expression in HEK293-hLAT2 cells was fairly high (lane 14), whereas it was hardly detected in HEK293-mock cells (lane 2) and HEK293-hLAT1 cells (lane 8). In addition, 4F2hc expression was increased in HEK293-hLAT2 cells (lanes 17). LAT3 and LAT4 were not detected in all the cell lines (lanes 3, 4, 9, 10, 15, and 16).

Western blot analysis was performed on the membrane fractions prepared from the HEK293-mock cells, HEK293-hLAT1 cells, HEK293-hLAT2 cells, and HeLa S3 cells. HeLa S3 was used as a positive control for the expression of LAT1 and 4F2hc. In the reducing condition, a single band slightly above the 35-kDa marker was detected by anti-LAT1 antibody in the HEK293-hLAT1 cells and HeLa S3 cells (Fig. 2B: left panel, lanes 2 and 4). The anti-LAT1 antibody recognized two bands approximately at 125 and 35 kDa under the non-reducing condition in HEK293-hLAT1 cells (Fig. 2B: left panel, lane 6) and a major band around 125 kDa in HeLa S3 cells (Fig. 2B: left panel, lane 8). Bands approximately at 125 kDa were also detected with anti-4F2hc antibody (Fig. 2B: right panel, lane 6), indicating that the upper bands correspond to the LAT1-4F2hc heterodimeric complex. Under the reducing condition, the lower LAT1 band approximately at 35 kDa was also observed marginally in the mock cells by increasing the amount of membrane proteins applied (data not shown). As shown in the middle panels of Fig. 2B, the anti-LAT2 antibody recognized a single band approximately at 45 kDa in the reducing condition (lane 3) and two bands around at 130 and 45 kDa in the non-reducing condition (lane 7) in HEK293-hLAT2 cells. The upper bands were recognized by anti-4F2hc antibody as well (Fig. 2B: right panel, lane 7) and disappeared under the reducing condition (Fig. 2B: right panel, lane 3). LAT2 was not detected in HEK293-mock, HEK293-hLAT1, and HeLa S3 cells (Fig. 2B: middle panel, lanes 1, 2, and 4). The sizes for LAT1, LAT2, and their heterodimers with 4F2hc were consistent with those reported previously (30, 39).

To confirm that the endogenous 4F2hc of HEK293 cells formed a heterodimer with exogenously expressed LAT1 or LAT2, the 4F2hc was immunoprecipitated by an anti-human 4F2hc monoclonal antibody (Fig. 2C). As shown in the right panel of Fig. 2C, the anti-4F2hc antibody successfully precipitated the endogenous 4F2hc from the HEK293-mock, HEK293-hLAT1, and HEK293-hLAT2 cells (lanes 4 – 6). Co-immunoprecipitated LAT1 was detected in the mock cells and predominantly in HEK293-hLAT1 cells (Fig. 2C: left panel, lanes 4 and 5), whereas precipitants from HEK293-hLAT2 cells showed a very faint signal of LAT1 (lane 6). Although LAT1 protein was hardly detected in HEK293-mock cells and HEK293-hLAT2 cells in the membrane fraction (Fig. 2B: left panel, lanes 1 and 3) and cell lysates (Fig. 2C: left panel, lanes 1 and 3), the accumulation of LAT1 by co-immunoprecipitation made LAT1 in both cells detectable (Fig. 2C: left panel, lanes 4 and 6). LAT2 was co-precipitated only from HEK293-hLAT2 cells, whereas the HEK293-mock and HEK293-hLAT1 cells showed no LAT2 band (Fig. 2C: middle panel, lanes 4 – 6). LAT1, LAT2, and 4F2hc were not co-precipitated with

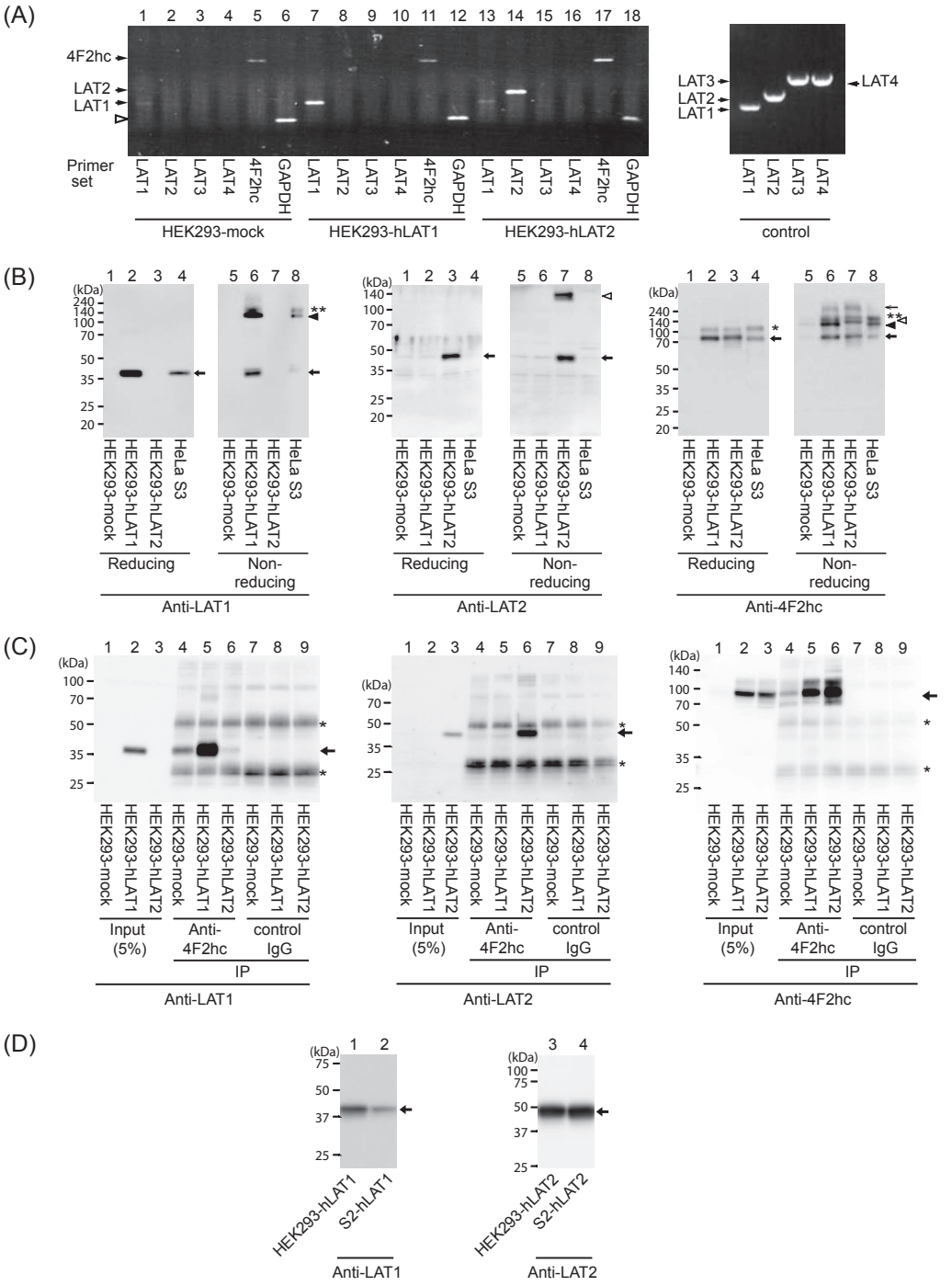

Fig. 2. Expression of LAT1 and LAT2 in HEK293-hLAT1 and HEK293-hLAT2 cells. A: Agarose gel electrophoresis showing RT-PCR products of LAT1, LAT2, LAT3, LAT4, and 4F2hc as well as GAPDH in HEK293-mock, HEK293-hLAT1, and HEK293-hLAT2 cells. An open arrow-head indicates the band corresponding to GAPDH. The right panel shows the bands of control PCR products obtained by amplification of cDNAs for human LAT1, LAT2, LAT3, and LAT4. GAPDH, glyceraldehyde-3-phosphate dehydrogenase. B: Western blot analysis of the crude membrane fraction prepared from HEK293-mock, HEK293-hLAT1, and HEK293-hLAT2 cells as well as HeLa S3 cells using antibodies against LAT1 (left panel), LAT2 (middle panel), and 4F2hc (right panel). Western blot was performed in the presence ("Reducing") or absence ("Non-reducing") of dithiothreitol. Thick arrows indicate the bands corresponding to the monomer of LAT1 in the left panel, that of LAT2 in the middle panel, or that of 4F2hc in the right panel. Filled arrowhead indicates the heterodimerization complex of LAT1 and 4F2hc, whereas the open arrowhead indicates that of LAT2 and 4F2hc. A single star represents an additional band for 4F2hc. Double stars presumably indicate heterodimers containing 4F2hc, which was indicated by the single star. A thin arrow appears to indicate aggregations of the complex. C: Co-immunoprecipitation using anti-4F2hc monoclonal antibody performed on HEK293-mock, HEK293-hLAT1, and HEK293-hLAT2 cells. In lanes 1 – 3, 5% of the total cell-lysate inputs used for the immunoprecipitation were applied. Arrows indicate the bands corresponding to LAT1, LAT2, and 4F2hc in the left, middle, and right panels, respectively. Stars indicate bands from IgG used for the immunoprecipitation. D: Western blot of plasma membrane fractions from HEK293-hLAT1 (lane 1), HEK293-hLAT2 (lane 3), S2-hLAT1 (lane 2), and S2-hLAT2 (lanes 4). The plasma membrane fractions were purified by using density gradient centrifugation and subjected to SDS-PAGE in the presence of dithiothreitol. Left panel was detected by anti-LAT1 antibody, whereas the right panel was detected by anti-LAT2 antibody.

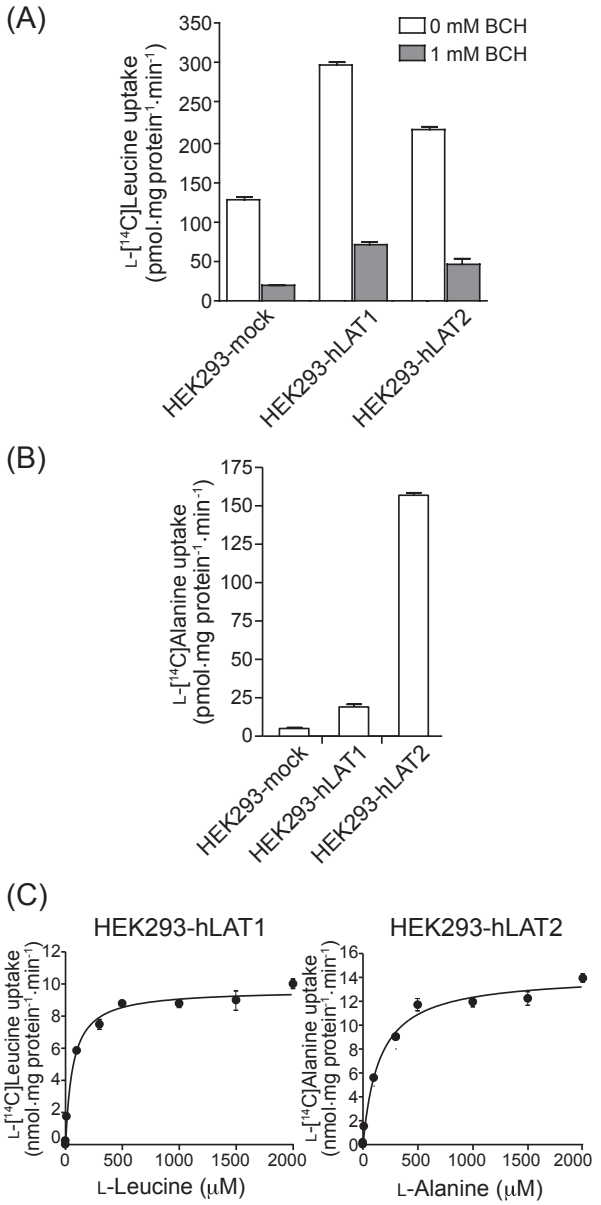

Fig. 3. Transport of amino acids in HEK293-hLAT1 and HEK293-hLAT2 cells. A: The uptake of L-[^{14}C]leucine (1.0 μM) by HEK293-mock, HEK293-hLAT1, and HEK293-hLAT2 cells in the absence (open column) or presence (closed column) of BCH (1.0 mM). B: The uptake of L-[^{14}C]alanine (1.0 μM) by HEK293-mock, HEK293-hLAT1, and HEK293-hLAT2 cells. C: Concentration-dependent uptake of L-[^{14}C]leucine in HEK293-hLAT1 cells and that of L-[^{14}C]alanine in HEK293-hLAT2 cells. The uptakes of L-[^{14}C]leucine (left) and L-[^{14}C]alanine (right) were measured at 1, 10, 100, 300, 500, 1000, 1500, and 2000 μM in HEK293-hLAT1 cells and HEK293-hLAT2 cells, respectively. The curves fit to the Michaelis-Menten equation. K_m values are described in Table 1. V_{max} value for L-[^{14}C]leucine uptake by HEK293-hLAT1 cells and that for L-[^{14}C]alanine uptake by HEK293-hLAT2 cells were 9.65 ± 0.2 nmol·mg protein^{-1}·min^{-1} and 14.2 ± 0.4 nmol·mg protein^{-1}·min^{-1}, respectively.

control IgG (lanes 7 – 9 in all panels of Fig. 2C).

The levels of expression of LAT1 and LAT2 on the plasma membrane were compared between stable cell lines established in the present study from HEK293 cells and those generated previously from S2 cells. As shown in Fig. 2D, HEK293-hLAT1 cells showed larger amount of LAT1 on the plasma membrane compared with S2-hLAT1 cells, whereas the level of LAT2 is similar between HEK293-hLAT2 cells and S2-hLAT2 cells (Fig. 2D).

Transport properties

The properties of the uptake of L-[^{14}C]leucine and L-[^{14}C]alanine were compared among HEK293-mock, HEK293-hLAT1, and HEK293-hLAT2 cells. L-[^{14}C]Leucine uptake of HEK293-hLAT1 and HEK293-hLAT2 cells was higher than that of HEK293-mock cells because the stable clones that exhibited higher L-[^{14}C]leucine uptake were selected in the screening of clones (Fig. 3A). The L-[^{14}C]leucine uptake of HEK293-mock, HEK293-hLAT1, and HEK293-hLAT2 cells was all inhibited by a classic system L inhibitor, 2-aminobicyclo-(2,2,1)-heptane-2-carboxylic acid (BCH) (Fig. 3A). In the present study, we, furthermore, measured L-[^{14}C]alanine uptake because L-alanine is a good substrate for LAT2 but not for LAT1 (3, 40). As indicated in Fig. 3B, HEK293-hLAT2 cells showed high level of L-[^{14}C]alanine uptake. In contrast, the L-[^{14}C]alanine uptake of HEK293-mock and HEK293-hLAT1 cells was quite low (Fig. 3B). The uptake of L-[^{14}C]leucine (1.0 μM) by HEK293-hLAT1 cells and that of L-[^{14}C]alanine (1.0 μM) by HEK293-hLAT2 cells both exhibited a linear dependence on the incubation time during the first 2 – 3 min (data not shown). Thus, all the uptake measurements were conducted for 1 min. The uptake of L-[^{14}C]leucine in HEK293-hLAT1 cells and that of L-[^{14}C]alanine in HEK293-hLAT2 cells were saturable and followed Michaelis-Menten kinetics (Fig. 3C). The kinetic parameters of the uptake were listed in Table 1. The uptake of L-[^{14}C]leucine in HEK293-mock cells was also fitted to a

Table 1. Kinetic parameters of amino acid–related compounds in HEK293-hLAT1 and HEK293-LAT2

	Compounds	K_m (μM)	K_i (μM)
HEK293-hLAT1	Leucine	64.5 ± 8.7	44.8 ± 5.3
	BCH		78.3 ± 12.1
	α-Methyl-L-tyrosine		90.7 ± 18.7
HEK293-hLAT2	Alanine	151.3 ± 17.7	119.0 ± 18.3
	BCH		150.5 ± 18.5
	α-Methyl-L-tyrosine		839.9 ± 123.4

Michaelis-Menten curve and showed a similar K_m value (56.3 μM) to that in HEK293-hLAT1 cells.

Inhibition of LAT1- and LAT2-mediated uptake by amino acids and their derivatives

The uptake of L-[^{14}C]leucine by HEK293-hLAT1 cells and that of L-[^{14}C]alanine (1.0 μM) by HEK293-hLAT2 cells were measured in the presence of 1.0 mM non-radiolabeled L-amino acids (Fig. 4). The uptake of L-[^{14}C]leucine by HEK293-hLAT1 cells was inhibited at higher levels by L-methionine, L-leucine, L-isoleucine, L-valine, L-phenylalanine, L-tyrosine, L-tryptophan, L-histidine, and BCH and at lower levels by L-alanine, L-serine, L-threonine, L-cysteine, L-asparagine, and L-glutamine (Fig. 4A). Glycine, L-proline, L-cystine, basic amino acids such as L-lysine and L-arginine, and acidic amino acids such as L-glutamate and L-aspartate caused little or no inhibition on L-[^{14}C]leucine uptake in HEK293-hLAT1 cells. The similar inhibition profile was obtained in the mock cells (data not shown). The L-[^{14}C]alanine uptake of HEK293-hLAT2 cells was strongly inhibited by all the neutral amino acids, L-histidine and BCH, whereas L-proline, L-cystine, L-lysine, L-arginine, L-glutamate, and L-aspartate did not inhibit L-[^{14}C]alanine uptake (Fig. 4B). It is noteworthy that both stably-transfected cell lines showed the same profiles of inhibition by amino acids even after 10 passages or recovering from frozen stocks in liquid nitrogen (data not shown).

Amino acid derivatives were also examined for the inhibitory effects on HEK293-hLAT1, and HEK293-hLAT2 cells. As shown in Fig. 5A, the ones with bulky side chains such as 3,3′,5-triiodothyronine (T3) and thyroxine (T4) (10 μM) inhibited the uptake of L-[^{14}C]leucine (1 μM) by HEK293-hLAT1 cells, whereas they did not inhibit the uptake of L-[^{14}C]alanine (1 μM) by HEK293-hLAT2 cells. The α-methyl amino acids such as α-methyl-L-tyrosine and α-methyl-L-phenylalanine (1.0 mM) strongly inhibited the uptake of L-[^{14}C]leucine (10 μM) in HEK293-hLAT1 cells, whereas they weakly inhibited the uptake of L-[^{14}C]alanine (10 μM) in HEK293-hLAT2 cells (Fig. 5B). The inhibition of L-[^{14}C]alanine uptake by α-methyl-L-DOPA in HEK293-hLAT2 cells was prominently less than that by L-DOPA (Fig. 5B). The level of inhibition was similar to that for α-methyl-L-tyrosine and α-methyl-L-phenylalanine in HEK293-hLAT2 cells, although the inhibition of L-[^{14}C]leucine uptake by α-methyl-L-DOPA in HEK293-hLAT1 cells was relatively less than that by α-methyl-L-tyrosine and α-methyl-L-phenylalanine (Fig. 5B). The effects of α-methyl-alanine and α-ethyl-L-alanine were examined on LAT2 because L-alanine is a good substrate of LAT2. The inhibition of L-[^{14}C]alanine uptake by α-methyl-alanine and α-ethyl-L-alanine in HEK293-hLAT2 cells was less than that by L-alanine (Fig. 5B). Furthermore, the inhibition by α-ethyl-L-alanine was significantly less than that by α-methyl-alanine ($P < 0.01$).

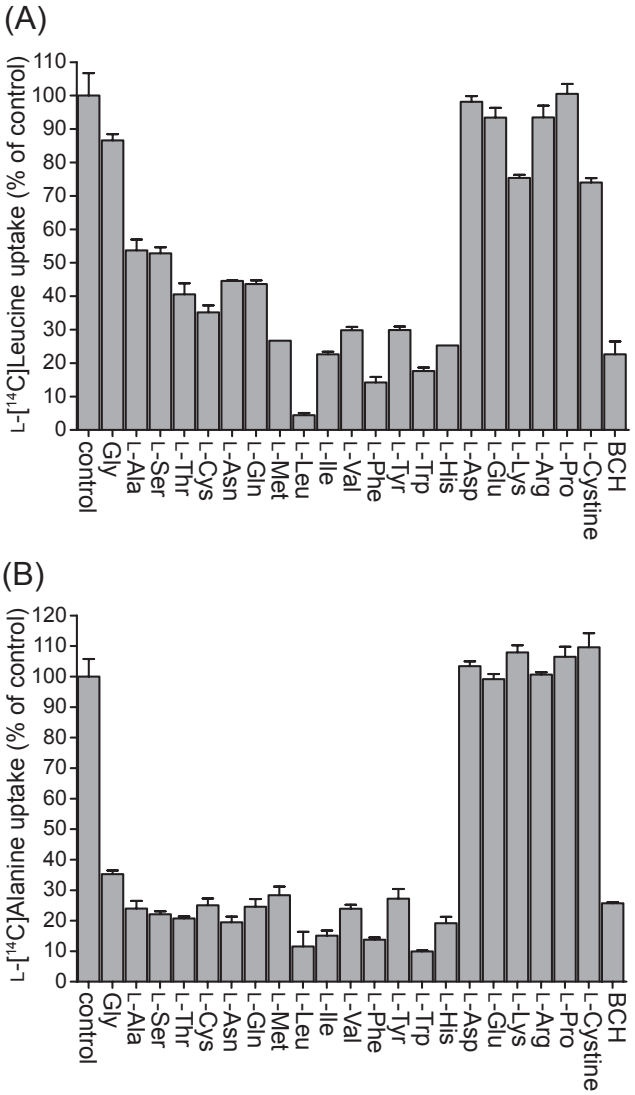

Fig. 4. Inhibition of L-[^{14}C]leucine uptake in HEK293-hLAT1 cells and that of L-[^{14}C]alanine uptake in HEK293-hLAT2 cells by amino acids. A: The uptake of L-[^{14}C]leucine (1.0 μM) was measured in the presence of 1.0 mM non-radiolabeled glycine, indicated L-amino acids, and BCH in HEK293-hLAT1 cells. B: The uptake of L-[^{14}C]alanine (1.0 μM) was measured in the presence of 1.0 mM non-radiolabeled glycine, indicated L-amino acids, and BCH in HEK293-hLAT2. The values are expressed as percent of the control L-[^{14}C]leucine or L-[^{14}C]alanine uptake measured in the absence of inhibitors.

Figure 6 illustrates the concentration-dependence of the inhibition of L-[^{14}C]leucine uptake in HEK293-hLAT1 cells and L-[^{14}C]alanine uptake in HEK293-hLAT2 cells. L-Leucine, BCH, and α-methyl-L-tyrosine inhibited LAT1-mediated L-[^{14}C]leucine uptake in a

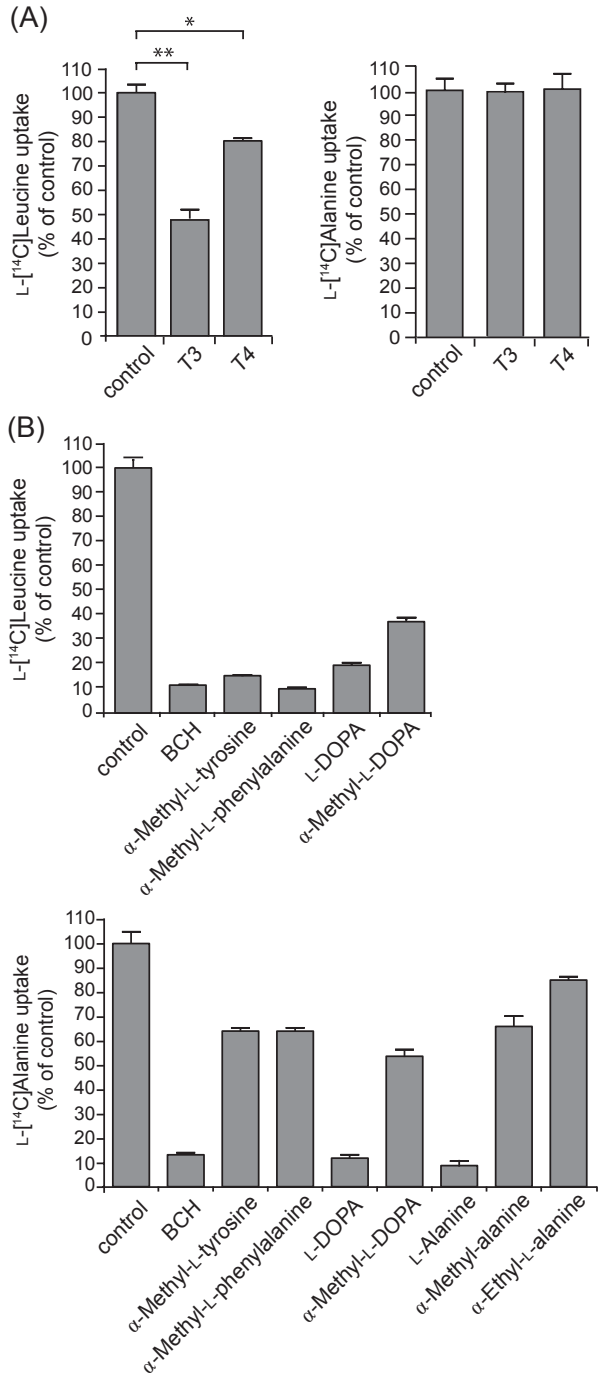

Fig. 5. The effects of amino acid derivatives on L-[^{14}C]leucine uptake in HEK293-hLAT1 cells and L-[^{14}C]alanine uptake in HEK293-hLAT2 cells. A: The uptake of L-[^{14}C]leucine (1.0 μM) in HEK293-hLAT1 cells (left) and that of L-[^{14}C]alanine (1.0 μM) in HEK293-hLAT2 cells (right) were measured in the absence ("control") or presence of non-radiolabeled inhibitors T3 and T4 (10 μM). *P < 0.05, **P < 0.01. T3, 3,3′,5-triiodothyronine; T4, thyroxine. B: The uptake of L-[^{14}C]leucine (10 μM) in HEK293-hLAT1 cells (upper) and that of L-[^{14}C]alanine (10 μM) in HEK293-hLAT2 cells (lower) were measured in the absence ("control") or presence of non-radiolabeled inhibitors (1 mM) as indicated. The values are expressed as percent of the control L-[^{14}C]leucine or L-[^{14}C]alanine uptake measured in the absence of inhibitors.

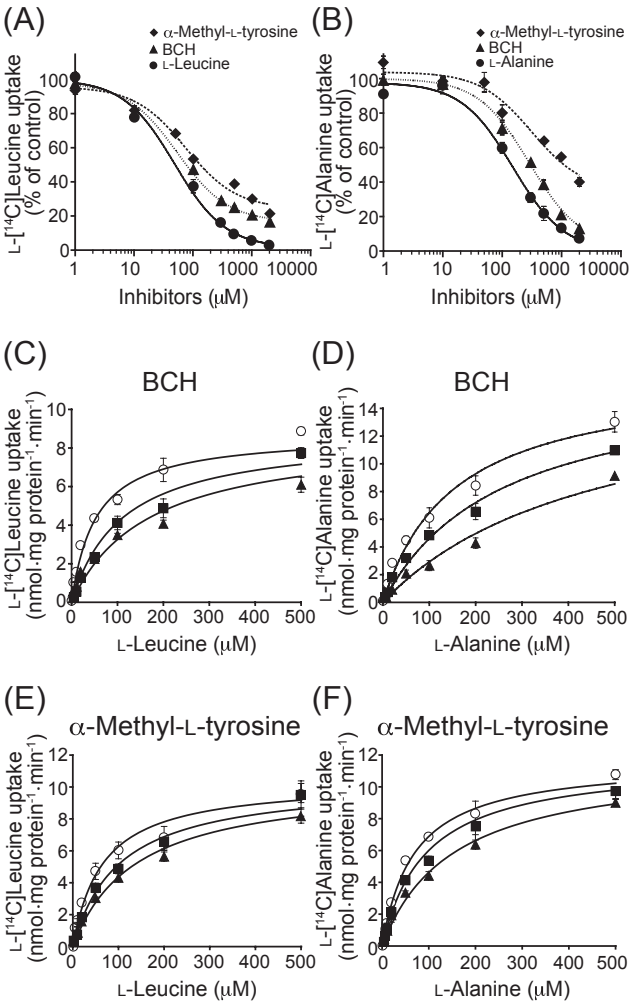

Fig. 6. Concentration-dependent profiles of the inhibition of L-[^{14}C]leucine uptake in HEK293-hLAT1 cells and those of the inhibition of L-[^{14}C]alanine uptake in HEK293-hLAT2 cells. A, B: Concentration-dependent inhibition of L-[^{14}C]leucine uptake by L-leucine (closed circles), BCH (closed triangles), and α-methyl-L-tyrosine (closed diamonds) in HEK293-hLAT1 cells (A) and that of L-[^{14}C]alanine uptake in HEK293-hLAT2 cells by L-alanine (closed circles), BCH (closed triangles), and α-methyl-L-tyrosine (closed diamonds) (B). The concentration of substrates L-[^{14}C]leucine and L-[^{14}C]alanine was 1.0 μM. The values are expressed as percent of the control L-[^{14}C]leucine or L-[^{14}C]alanine uptake measured in the absence of inhibitors. C – F: The effects of BCH and α-methyl-L-tyrosine on the concentration-dependent uptake of L-[^{14}C]leucine in HEK293-hLAT1 cells (C, E) and on the L-[^{14}C]alanine uptake in HEK293-hLAT2 cells (D, F). The uptake of L-[^{14}C]leucine in HEK293-hLAT1 cells and that of L-[^{14}C]alanine in HEK293-hLAT2 cells were measured at 1, 5, 10, 20, 50, 100, 200, and 500 μM. Concentrations of inhibitors used were 0 (open circles), 50 (closed squares), and 100 (closed triangles) μM for both BCH (C) and α-methyl-L-tyrosine (E) in HEK293-hLAT1 cells. In HEK293-hLAT2 cells, concentrations of inhibitors used for BCH (D) were 0 (open circles), 100 (closed squares), and 300 (closed triangles) μM, whereas those for α-methyl-L-tyrosine (F) were 0 (open circles), 300 (closed squares), and 1,000 (closed triangles) μM.

concentration-dependent manner (Fig. 6A). Similarly, L-alanine, BCH, and α-methyl-L-tyrosine concentration-dependently inhibited LAT2-mediated L-[^{14}C]alanine uptake (Fig. 6B). IC_{50} values of L-leucine, BCH, and α-methyl-L-tyrosine to inhibit L-[^{14}C]leucine uptake in HEK293-hLAT1 were 48.5, 53.9, and 75.4 μM, respectively. As for HEK293-hLAT2 cells, IC_{50} values of L-alanine, BCH, and α-methyl-L-tyrosine to inhibit L-[^{14}C]alanine uptake were 151.7, 289.9, and 312.9 μM, respectively. The effects of BCH and α-methyl-L-tyrosine were further examined on the concentration dependence of LAT1-mediated L-[^{14}C]leucine uptake and LAT2-mediated L-[^{14}C]alanine uptake. As shown in Fig. 6, C – F, BCH and α-methyl-L-tyrosine shifted the concentration-dependence curves for both LAT1-mediated L-[^{14}C]leucine uptake and LAT2-mediated L-[^{14}C]alanine uptake. The inhibition kinetics of both BCH and α-methyl-L-tyrosine as well as L-leucine and L-alanine fit to the competitive inhibition by non-linear regression analysis, which was also confirmed by Lineweaver-Burk plots (data not shown). K_i values are listed in Table 1. K_i value of α-methyl-L-tyrosine for LAT2 was approximately 9-fold of that for LAT1.

Discussion

In this study, to establish the human cell lines stably expressing human LAT1 and human LAT2, we used HEK293 cells as host cells because endogenous LAT1 expression of HEK293 cells is lower than that of most human cell lines generally available in laboratories (data not shown). This property is beneficial to reduce the backgrounds of amino acid transport and to avoid the contamination of endogenous LAT1 activity particularly in LAT2-transfected cells. It was confirmed by RT-PCR and western blotting using antibodies against LAT1 and LAT2 that the exogenously transfected LAT1 and LAT2 were expressed at high level in HEK293 cells (Fig. 2: A and B). In fact, the LAT1 protein level of HEK293-hLAT1 cells was higher than that of HeLa S3 (Fig. 2B), one of the cell lines with the highest LAT1 expression. Furthermore, predominant bands corresponding to the heterodimers of exogenously introduced LAT1 or LAT2 with endogenous 4F2hc of HEK293 cells were detected in non-reducing condition (Fig. 2B). LAT1 and LAT2 were co-immunoprecipitated using the anti-4F2hc antibody (Fig. 2C). This suggests that exogenously introduced LAT1 and LAT2 appear on the cell surface by forming heterodimers with endogenous 4F2hc, which is essential for cell surface localization of LAT1 and LAT2 (2, 3, 15). Because of the overexpression of exogenously introduced LAT1 and LAT2, endogenous LAT1 of HEK293 cells would be competed out and not be able to form heterodimers with 4F2hc, so that exogenously introduced LAT1 or LAT2 would be predominant as partners of 4F2hc on the plasma membrane. Therefore, the cell lines we generated in the present study are proposed to almost exclusively express exogenously introduced LAT1 or LAT2 as the partner of endogenous 4F2hc on the cell surface with avoiding surface expression of endogenous LAT1 of HEK293 cells. This is also advantageous considering the formation of heterodimers between human 4F2hc and human LAT1 or LAT2, compared with S2-hLAT1 and S2-hLAT2 cells generated previously using a mouse cell line in which heterodimers of mouse 4F2hc and human LAT1 or LAT2 are formed (30). Although the contribution of 4F2hc to the function of partner transporters has not been defined at the moment, the heterodimers of human LAT1 or LAT2 with human 4F2hc would be more desirable to evaluate the functions of human LAT1 and LAT2.

The clones of HEK293-hLAT1 and HEK293-hLAT2 cells that we selected in screening for higher uptake of substrates showed high levels of expression of LAT1 or LAT2. The level of expression of LAT1 in the plasma membrane fraction of HEK293-hLAT1 cells was much higher than that of S2-hLAT1 cells (Fig. 2D). The level of expression of LAT2 in the plasma membrane fraction of HEK293-hLAT2 cells was similar to that of S2-hLAT2 cells which highly express LAT2 (Fig. 2D). In the screening of cell clones with higher substrate uptake function, we were eventually able to obtain the clones with quite high 4F2hc protein levels (Fig. 2B), which could explain the reason why the cell clones with higher surface LAT1 and LAT2 levels were obtained. In addition to the aforementioned benefit of forming heterodimers between human 4F2hc and human LAT1 or LAT2, HEK293-hLAT1 and HEK293-hLAT2 cells established in the present study, compared with previously generated S2-hLAT1 and S2-hLAT2 cells (30), have the benefits of lower background of LAT1 in host HEK293 cells, higher level of expression of transfected LAT1 on the cell surface, easier handling of the established cell lines due to simple conventional culture medium required for the maintenance of the cells, and somewhat more stable expression of transfected LAT1 and LAT2. Such properties would be advantageous when HEK293-hLAT1 and HEK293-hLAT2 cells are used for the screening of chemical compounds interacting with LAT1 or LAT2 as well as in the kinetic analysis of their interactions.

In the previous studies conducted on S2-hLAT1 and S2-hLAT2 cells, we used L-[^{14}C]leucine as a substrate to characterize the functional properties of the stably expressing cell lines and to examine the interaction of chemical compounds with both LAT1 and LAT2 (18, 30). Because the host or mock cells take up L-[^{14}C]leucine

due to the endogenous LAT1-4F2hc complex on the plasma membrane and also because LAT2-specific inhibitors were not presently available, it was difficult for LAT2-expressing cells to evaluate the contribution of exogenously expressed LAT2 to L-[^{14}C]leucine uptake of the cells. In this study, we have found that L-[^{14}C]alanine is an appropriate substrate to evaluate the function of exogenously expressed LAT2 in HEK293 cells. L-[^{14}C]alanine uptake of the mock or host HEK293 cells was quite low, whereas HEK293-hLAT2 cells exhibited remarkably high L-[^{14}C]alanine uptake (Fig. 3B). In contrast, L-[^{14}C]alanine uptake by HEK293-hLAT1 cells was low (Fig. 3B). This clearly indicates that L-[^{14}C]alanine is specific to LAT2 in HEK293 cells in a Na^+-free condition so that L-[^{14}C]alanine is a desirable substrate for evaluating the function of LAT2 introduced into HEK293 cells. By using HEK293-hLAT2 cells and L-[^{14}C]alanine as a substrate in the present study, we have succeeded for the first time to evaluate directly the function of human LAT2 expressed in mammalian cells and to obtain its reliable kinetic parameters for the transport.

The K_m value of LAT2 for L-alanine uptake determined in this study using HEK293-hLAT2 cells (151 μM) agrees with that reported for LAT2 expressed in *Xenopus* oocyte (187 μM) (3). Similarly, the K_m value for L-leucine measured on HEK293-hLAT2 cells (153 μM), rather than that reported for S2-hLAT2 cells (318.0 μM) (30), corresponds more to that obtained using the *Xenopus* oocyte expression system (119 μM) (3). We propose that L-[^{14}C]alanine uptake measurement on HEK293-hLAT2 cells should enable the accurate functional evaluation of LAT2 in culture cells and the reliable estimation of the interaction of chemical compounds with LAT2. Inhibition profiles of HEK293-hLAT1 cells and HEK293-hLAT2 cells obtained in this study (Fig. 4: A and B) are basically similar to those reported previously for LAT1 and LAT2 examined in *Xenopus* oocytes (2, 3, 5). This is consistent with the idea that endogenous 4F2hc of HEK293 cells is associated with exogenously introduced LAT1 and LAT2 in the HEK293-hLAT1 and HEK293-hLAT2 cells, respectively. Thus, the transport function of these stably transfected HEK293 cell lines reflects the properties of exogenously introduced LAT1 and LAT2.

As reported for S2-hLAT1 and S2-hLAT2 cells and for *Xenopus* oocyte expression systems (21, 30), thyroid hormones, T3 and T4, and α-methyl aromatic amino acids such as α-methyl-L-tyrosine, α-methyl-L-phenylalanine, and α-methyl-L-DOPA are more selective to LAT1 compared with LAT2 in HEK293-hLAT1 and HEK293-hLAT2 cells (Fig. 5: A and B). In the experimental scheme that we validated in the present study, we measured kinetic parameters of α-methyl-L-tyrosine for human LAT1 and human LAT2. α-Methyl-L-tyrosine inhibited both human LAT1 and human LAT2 in a concentration-dependent manner with K_i values of 90.7 μM and 839.9 μM, respectively (Fig. 6 and Table 1). This demonstrates for the first time in a quantitative manner that α-methyl-L-tyrosine is selective to LAT1. In this study, we furthermore, examined the effect of a wider spectrum of α-alkyl amino acids including α-methyl-alanine and α-ethyl-L-alanine, which have not been studied so far. We confirmed that LAT1 interacts with the α-methyl moiety (Fig. 5B). In contrast, LAT2 less interacted with α-alkyl moieties. Although L-alanine strongly inhibited LAT2-mediated uptake, its α-alkyl derivatives such as α-methyl-alanine and α-ethyl-L-alanine inhibited LAT2 very weakly (Fig. 5B). α-Ethyl-L-alanine interacted less with LAT2 compared with α-methyl-alanine, suggesting that bulkiness at the α-position interferes with the interaction with LAT2. Thus, the nature of LAT2 which does not accept the α-methyl moiety was further confirmed by using α-alkyl derivatives of LAT2 substrates. It was also the first demonstration that the α-ethyl group interferes with the interaction of amino acids with LAT2.

In this study, we also measured K_i values of BCH on LAT1 and LAT2 in HEK293-hLAT1 and HEK293-hLAT2 cells to show that BCH is more selective to LAT1 compared with LAT2 (Fig. 6 and Table 1). Since BCH was originally developed as a system L inhibitor by Christensen and co-workers (1), the differential sensitivity of system L isoforms to BCH has not been considered quantitatively. BCH has been in fact regarded as a general inhibitor of system L (1). In the previous study using S2-hLAT1 and S2-hLAT2 cells, we examined the effect of BCH on LAT1 and LAT2 and obtained the K_i values to indicate that BCH is more selective to LAT1 than LAT2 (30). Now we have confirmed it in the experimental scheme validated in the present study and concluded the LAT1-selectivity of BCH. In in vivo studies in which BCH was used to inhibit LAT1 expressed in cancers, BCH suppressed cancer growth with less side effects (12). This could be explained by the LAT1-selective nature of BCH.

It has been shown that LAT1 is upregulated in tumor cells to supply tumor cells with amino acids to support their continuous growth and proliferation (2, 7 – 20, 41). In contrast, LAT2 is essential for the amino acid supply to non-cancer cells and for the epithelial transport of amino acids in the small intestine and kidney (3, 25). Therefore, the development of LAT1-specific inhibitors or substrates that do not affect LAT2 should have important therapeutic and diagnostic implications. The LAT1-selective inhibitors would suppress tumor cell growth by reducing amino acid supply to tumor cells so that they

could be used as anti-tumor agents with less side effects on non-tumor cells. Furthermore, LAT1-selective substrates are expected to be selectively taken up and accumulate in tumor cells so that it could be used as probes for cancer diagnosis in PET and single photon emission computed tomography (SPECT). L-[3-^{18}F]Fluoro-α-methyl-tyrosine ([^{18}F]FAMT) (9) and L-[3-^{123}I]iodo-α-methyl-tyrosine ([^{123}I]IMT) (42, 43), LAT1-selective α-methyl aromatic amino acids, have been used for PET and SPECT, respectively (24). These LAT1-selective radiotracers are quite beneficial compared with the conventionally used glucose analogue PET tracer 2-[^{18}F]fluoro-2-deoxy-D-glucose ([^{18}F]FDG) and other amino acid PET tracers in the differentiation of malignant tumors and benign lesions as well as in reducing physiological backgrounds in the imaging (22, 24, 44, 45). LAT1-selective substrates could also be used for the treatment of cancers if the compounds are taken up by the cells via LAT1 and exert anti-tumor effects: melphalan, a phenylalanine mustard, and borono-phenylalanine used for boron neutron capture therapy (19, 23). For the delivery of amino acid-related drugs though the blood–brain barrier, it would be advantageous to design drugs to be transported by both LAT1 and LAT2 which exist in the barriers. The in vitro simple assay systems developed and validated in this study would be useful for generating such drugs interacting with LAT1 and/or LAT2.

In summary, we have established human cell lines stably expressing high level of heterodimeric complexes of human 4F2hc and human amino acid transporter LAT1 or LAT2 on the cell surface. We have, furthermore, established reliable assays to investigate the interaction of the transporters with chemical compounds. These cell lines that can be maintained in the conventional culture medium could also be used for the screening of compounds to develop drugs specific to LAT1 and/or LAT2 with desired pharmacodynamics and pharmacokinetics. In addition, the strategy we took in this study to establish cell lines stably expressing heterodimeric transporters would also be applicable to the other heterodimeric transporters. The drugs targeting xCT1 and Asc-1, members of the heterodimeric transporters, would also have important clinical implications (46, 47).

Acknowledgments

This work was supported in part by a Grant-in-Aid for Scientific Research on Priority Areas of 'Transportsome' from the Ministry of Education, Culture, Sports, Science, and Technology of Japan and Grants-in-Aid for Scientific Research from the Japan Society for the Promotion of Science, the Osaka Medical Research Foundation for Intractable Diseases, Hyogo COE Program Promotion Project, and Ajinomoto Amino Acid Research Program. The authors are grateful to Michiko Minobe for technical assistance.

References

1 Christensen HN. Role of amino acid transport and countertransport in nutrition and metabolism. Physiol Rev. 1990;70:43–77.
2 Kanai Y, Segawa H, Miyamoto K, Uchino H, Takeda E, Endou H. Expression cloning and characterization of a transporter for large neutral amino acids activated by the heavy chain of 4F2 antigen (CD98). J Biol Chem. 1998;273:23629–23632.
3 Segawa H, Fukasawa Y, Miyamoto K, Takeda E, Endou H, Kanai Y. Identification and functional characterization of a Na^+-independent neutral amino acid transporter with broad substrate selectivity. J Biol Chem. 1999;274:19745–19751.
4 Verrey F, Closs EI, Wagner CA, Palacin M, Endou H, Kanai Y. CATs and HATs: the SLC7 family of amino acid transporters. Pflugers Arch. 2004;447:532–542.
5 Yanagida O, Kanai Y, Chairoungdua A, Kim DK, Segawa H, Nii T, et al. Human L-type amino acid transporter 1 (LAT1): characterization of function and expression in tumor cell lines. Biochim Biophys Acta. 2001;1514:291–302.
6 Matsuo H, Tsukada S, Nakata T, Chairoungdua A, Kim DK, Cha SH, et al. Expression of a system L neutral amino acid transporter at the blood-brain barrier. Neuroreport. 2000;11:3507–3511.
7 Kaira K, Oriuchi N, Imai H, Shimizu K, Yanagitani N, Sunaga N, et al. Prognostic significance of L-type amino acid transporter 1 (LAT1) and 4F2 heavy chain (CD98) expression in stage I pulmonary adenocarcinoma. Lung Cancer. 2009;66:120–126.
8 Kaira K, Oriuchi N, Imai H, Shimizu K, Yanagitani N, Sunaga N, et al. Prognostic significance of L-type amino acid transporter 1 expression in resectable stage I-III nonsmall cell lung cancer. Br J Cancer. 2008;98:742–748.
9 Kaira K, Oriuchi N, Shimizu K, Imai H, Tominaga H, Yanagitani N, et al. Comparison of L-type amino acid transporter 1 expression and L-[3-^{18}F]-alpha-methyl tyrosine uptake in outcome of non-small cell lung cancer. Nucl Med Biol. 2010;37:911–916.
10 Kaira K, Oriuchi N, Shimizu K, Tominaga H, Yanagitani N, Sunaga N, et al. ^{18}F-FMT uptake seen within primary cancer on PET helps predict outcome of non-small cell lung cancer. J Nucl Med. 2009;50:1770–1776.
11 Sakata T, Ferdous G, Tsuruta T, Satoh T, Baba S, Muto T, et al. L-type amino-acid transporter 1 as a novel biomarker for high-grade malignancy in prostate cancer. Pathol Int. 2009;59:7–18.
12 Nawashiro H, Otani N, Shinomiya N, Fukui S, Ooigawa H, Shima K, et al. L-type amino acid transporter 1 as a potential molecular target in human astrocytic tumors. Int J Cancer. 2006;119:484–492.
13 Kobayashi K, Ohnishi A, Promsuk J, Shimizu S, Kanai Y, Shiokawa Y, et al. Enhanced tumor growth elicited by L-type amino acid transporter 1 in human malignant glioma cells. Neurosurgery. 2008;62:493–503; discussion 503–504.
14 Fuchs BC, Bode BP. Amino acid transporters ASCT2 and LAT1 in cancer: partners in crime? Semin Cancer Biol. 2005;15:254–266.
15 Kanai Y, Endou H. Heterodimeric amino acid transporters: molecular biology and pathological and pharmacological relevance. Curr Drug Metab. 2001;2:339–354.
16 Yamauchi K, Sakurai H, Kimura T, Wiriyasermkul P, Nagamori S, Kanai Y, et al. System L amino acid transporter inhibitor enhances anti-tumor activity of cisplatin in a head and neck

squamous cell carcinoma cell line. Cancer Lett. 2009;276: 95–101.
17 Nicklin P, Bergman P, Zhang B, Triantafellow E, Wang H, Nyfeler B, et al. Bidirectional transport of amino acids regulates mTOR and autophagy. Cell. 2009;136:521–534.
18 Oda K, Hosoda N, Endo H, Saito K, Tsujihara K, Yamamura M, et al. L-type amino acid transporter 1 inhibitors inhibit tumor cell growth. Cancer Sci. 2010;101:173–179.
19 Kim DK, Kanai Y, Choi HW, Tangtrongsup S, Chairoungdua A, Babu E, et al. Characterization of the system L amino acid transporter in T24 human bladder carcinoma cells. Biochim Biophys Acta. 2002;1565:112–121.
20 Kanai Y, Endou H. Functional properties of multispecific amino acid transporters and their implications to transporter-mediated toxicity. J Toxicol Sci. 2003;28:1–17.
21 Uchino H, Kanai Y, Kim DK, Wempe MF, Chairoungdua A, Morimoto E, et al. Transport of amino acid-related compounds mediated by L-type amino acid transporter 1 (LAT1): insights into the mechanisms of substrate recognition. Mol Pharmacol. 2002;61:729–737.
22 Kaira K, Oriuchi N, Otani Y, Shimizu K, Tanaka S, Imai H, et al. Fluorine-18-alpha-methyltyrosine positron emission tomography for diagnosis and staging of lung cancer: a clinicopathologic study. Clin Cancer Res. 2007;13:6369–6378.
23 Detta A, Cruickshank GS. L-amino acid transporter-1 and boronophenylalanine-based boron neutron capture therapy of human brain tumors. Cancer Res. 2009;69:2126–2132.
24 Wiriyasermkul P, Nagamori S, Tominaga H, Oriuchi N, Kaira K, Nakao H, et al. Transport of 3-fluoro-L-α-methyl tyrosine by tumor-upregulated amino acid transporter LAT1: a cause of the tumor uptake in PET. J Nucl Med. In press.
25 Rossier G, Meier C, Bauch C, Summa V, Sordat B, Verrey F, et al. LAT2, a new basolateral 4F2hc/CD98-associated amino acid transporter of kidney and intestine. J Biol Chem. 1999; 274:34948–34954.
26 Broer S. Amino acid transport across mammalian intestinal and renal epithelia. Physiol Rev. 2008;88:249–286.
27 Roos S, Kanai Y, Prasad PD, Powell TL, Jansson T. Regulation of placental amino acid transporter activity by mammalian target of rapamycin. Am J Physiol Cell Physiol. 2009;296:C142–C150.
28 Loubiere LS, Vasilopoulou E, Bulmer JN, Taylor PM, Stieger B, Verrey F, et al. Expression of thyroid hormone transporters in the human placenta and changes associated with intrauterine growth restriction. Placenta. 2010;31:295–304.
29 Kido Y, Tamai I, Uchino H, Suzuki F, Sai Y, Tsuji A. Molecular and functional identification of large neutral amino acid transporters LAT1 and LAT2 and their pharmacological relevance at the blood-brain barrier. J Pharm Pharmacol. 2001;53:497–503.
30 Morimoto E, Kanai Y, Kim DK, Chairoungdua A, Choi HW, Wempe MF, et al. Establishment and characterization of mammalian cell lines stably expressing human L-type amino acid transporters. J Pharmacol Sci. 2008;108:505–516.
31 Kim DK, Kanai Y, Choi HW, Tangtrongsup S, Chairoungdua A, Babu E, et al. Characterization of the system L amino acid transporter in T24 human bladder carcinoma cells. Biochim Biophys Acta. 2002;1565:112–121.
32 Kurayama R, Ito N, Nishibori Y, Fukuhara D, Akimoto Y, Higashihara E, et al. Role of amino acid transporter LAT2 in the activation of mTORC1 pathway and the pathogenesis of crescentic glomerulonephritis. Lab Invest. 2011;91:992–1006.
33 Takeda M, Sekine T, Endou H. Regulation by protein kinase C of organic anion transport driven by rat organic anion transporter 3 (rOAT3). Life Sci. 2000;67:1087–1093.
34 Graham FL, Smiley J, Russell WC, Nairn R. Characteristics of a human cell line transformed by DNA from human adenovirus type 5. J Gen Virol. 1977;36:59–74.
35 Babu E, Takeda M, Nishida R, Noshiro-Kofuji R, Yoshida M, Ueda S, et al. Interactions of human organic anion transporters with aristolochic acids. J Pharmacol Sci. 2010;113:192–196.
36 Choi KS, Aizaki H, Lai MM. Murine coronavirus requires lipid rafts for virus entry and cell-cell fusion but not for virus release. J Virol. 2005;79:9862–9871.
37 Miyamoto N, Higuchi Y, Tsurudome M, Ito M, Nishio M, Kawano M, et al. Induction of c-Src in human blood monocytes by anti-CD98/FRP-1 mAb in an Sp1-dependent fashion. Cell Immunol. 2000;204:105–113.
38 Sakamoto S, Chairoungdua A, Nagamori S, Wiriyasermkul P, Promchan K, Tanaka H, et al. A novel role of the C-terminus of $b^{0,+}$AT in the ER-Golgi trafficking of the rBAT-$b^{0,+}$AT heterodimeric amino acid transporter. Biochem J. 2009;417:441–448.
39 Yanagida O, Kanai Y, Chairoungdua A, Kim DK, Segawa H, Nii T, et al. Human L-type amino acid transporter 1 (LAT1): characterization of function and expression in tumor cell lines. Biochim Biophys Acta. 2001;1514:291–302.
40. Broer S, Broer A, Hansen JT, Bubb WA, Balcar VJ, Nasrallah FA, et al. Alanine metabolism, transport, and cycling in the brain. J Neurochem. 2007;102:1758–1770.
41 Nawashiro H, Otani N, Uozumi Y, Ooigawa H, Toyooka T, Suzuki T, et al. High expression of L-type amino acid transporter 1 in infiltrating glioma cells. Brain Tumor Pathol. 2005;22: 89–91.
42 Shikano N, Kanai Y, Kawai K, Inatomi J, Kim DK, Ishikawa N, et al. Isoform selectivity of 3-^{125}I-iodo-alpha-methyl-L-tyrosine membrane transport in human L-type amino acid transporters. J Nucl Med. 2003;44:244–246.
43 Shikano N, Kanai Y, Kawai K, Ishikawa N, Endou H. Characterization of 3-[^{125}I]iodo-alpha-methyl-L-tyrosine transport via human L-type amino acid transporter 1. Nucl Med Biol. 2003; 30:31–37.
44 Kaira K, Oriuchi N, Shimizu K, Ishikita T, Higuchi T, Imai H, et al. Evaluation of thoracic tumors with ^{18}F-FMT and ^{18}F-FDG PET-CT: a clinicopathological study. Int J Cancer. 2009;124: 1152–1160.
45 Rosenbaum SJ, Lind T, Antoch G, Bockisch A. False-positive FDG PET uptake--the role of PET/CT. Eur Radiol. 2006;16: 1054–1065.
46 Fukasawa Y, Segawa H, Kim JY, Chairoungdua A, Kim DK, Matsuo H, et al. Identification and characterization of a Na^+-independent neutral amino acid transporter that associates with the 4F2 heavy chain and exhibits substrate selectivity for small neutral D- and L-amino acids. J Biol Chem. 2000;275:9690–9698.
47 Ishimoto T, Nagano O, Yae T, Tamada M, Motohara T, Oshima H, et al. CD44 variant regulates redox status in cancer cells by stabilizing the xCT subunit of system xc(-) and thereby promotes tumor growth. Cancer Cell. 2011;19:387–400.